Missouri University of Science and Technology
Scholars' Mine

Mechanical and Aerospace Engineering Faculty Research & Creative Works

Mechanical and Aerospace Engineering

01 May 2021

The Effect of Nanostructures in Aluminum Alloys Processed using Additive Manufacturing on Microstructural Evolution and Mechanical Performance Behavior

Rachel Boillat

Sriram Praneeth Isanaka
Missouri University of Science and Technology, sihyd@mst.edu

Frank W. Liou
Missouri University of Science and Technology, liou@mst.edu

Follow this and additional works at: https://scholarsmine.mst.edu/mec_aereng_facwork

 Part of the Mechanical Engineering Commons

Recommended Citation

R. Boillat et al., "The Effect of Nanostructures in Aluminum Alloys Processed using Additive Manufacturing on Microstructural Evolution and Mechanical Performance Behavior," *Crystals*, vol. 11, no. 5, MDPI, May 2021.
The definitive version is available at https://doi.org/10.3390/cryst11050524

This work is licensed under a Creative Commons Attribution 4.0 License.

This Article - Journal is brought to you for free and open access by Scholars' Mine. It has been accepted for inclusion in Mechanical and Aerospace Engineering Faculty Research & Creative Works by an authorized administrator of Scholars' Mine. This work is protected by U. S. Copyright Law. Unauthorized use including reproduction for redistribution requires the permission of the copyright holder. For more information, please contact scholarsmine@mst.edu.

crystals

MDPI

Review

The Effect of Nanostructures in Aluminum Alloys Processed Using Additive Manufacturing on Microstructural Evolution and Mechanical Performance Behavior

Rachel Boillat *, Sriram Praneeth Isanaka and Frank Liou

Department of Mechanical Engineering, Missouri University of Science and Technology, Rolla, MO 65409, USA; sihyd@mst.edu (S.P.I.); liou@mst.edu (F.L.)
* Correspondence: rmb8t6@mst.edu

Abstract: This paper reviews the status of nanoparticle technology as it relates to the additive manufacturing (AM) of aluminum-based alloys. A broad overview of common AM processes is given. Additive manufacturing is a promising field for the advancement of manufacturing due to its ability to yield near-net-shaped components that require minimal post-processing prior to end-use. AM also allows for the fabrication of prototypes as well as economical small batch production. Aluminum alloys processed via AM would be very beneficial to the manufacturing industry due to their high strength to weight ratio; however, many of the conventional alloy compositions have been shown to be incompatible with AM processing methods. As a result, many investigations have looked to methods to improve the processability of these alloys. This paper explores the use of nanostructures to enhance the processability of aluminum alloys. It is concluded that the addition of nanostructures is a promising route for modification of existing alloys and may be beneficial to other powder-based processes.

Keywords: additive manufacturing; nanoparticles; aluminum; microstructural features; mechanical properties; selective laser melting; directed energy deposition

check for updates

Citation: Boillat, R.; Isanaka, S.P.; Liou, F. The Effect of Nanostructures in Aluminum Alloys Processed Using Additive Manufacturing on Microstructural Evolution and Mechanical Performance Behavior. *Crystals* **2021**, *11*, 524. https://doi.org/10.3390/cryst11050524

Academic Editors: Hongbin Bei and Pavel Lukáč

Received: 30 March 2021
Accepted: 1 May 2021
Published: 8 May 2021

Publisher's Note: MDPI stays neutral with regard to jurisdictional claims in published maps and institutional affiliations.

Copyright: © 2021 by the authors. Licensee MDPI, Basel, Switzerland. This article is an open access article distributed under the terms and conditions of the Creative Commons Attribution (CC BY) license (https://creativecommons.org/licenses/by/4.0/).

1. Introduction

Additive manufacturing (AM) is an additive process that allows for the fabrication of near-net-shape 3D components that require minimal post-processing. As an additive process rather than a subtractive process, AM minimizes material waste and tooling costs commonly seen with subtractive processes. In addition, additive processes have garnered attention for the ability to produce complex geometries. Several industries, such as aerospace, have many components with complex geometries that would involve significant material waste, tooling, assembly, and labor-intensive practices, making them expensive if approached with subtractive methods.

Aluminum alloys are known for having a high strength to weight ratio, making them highly desirable for end-use in many structural applications, such as aerospace and automotive. As a result, there are several benefits to the ability to implement aluminum alloys with AM fabrication techniques; however, despite the benefits that can be gained, there are considerable issues that act as a barrier to successful implementation. Aluminum alloys that fall into the 2XXX, 5XXX, 6XXX, and 7XXX series are often characterized as having superior mechanical characteristics [1–5]; however, these alloys also suffer from solidification cracking as a result of a wide solidification range and other defect mechanisms common to AM and aluminum alloys [6–10]. Al 4XXX series alloys, often used with welding applications, have shown considerable success with AM [11–15], but the Al-Si system is not characterized as having high mechanical properties as compared with the other systems [1,2,16,17]. Additionally, aluminum alloys have been shown to suffer from vaporization of low boiling elements [6,18–20] along with issues inherent to the actual

process itself, such as high reflectivity [5,15,21], thermal conductivity [15,21], and oxide formation [21].

As a result of the difficulties surrounding the fabrication of components via AM processes, investigators have searched for ways to address the various problems, such as parameter optimization [10,22], alloy composition modification [23–25], and post-processing [12,14] to both resolve defects and promote fabrication of high mechanical property components. One solution of considerable interest is to utilize nanostructures as part of the feedstock material [8,26]. This review seeks to present the theories behind the use of nanostructures for AM of aluminum alloys and the current status of the implementation and results of nanostructure modified alloys.

1.1. Additive Manufacturing Processes

For metal AM using powder feedstock, the two main techniques fall into the category of either powder bed or powder fed. Powder bed AM is a process in which an energy source, most commonly a laser beam, selectively melts the preplaced powder in a powder bed to form a single cross-sectional layer of a 3D component. Selective laser melting (SLM) is one of the most common powder bed processes, Figure 1A. After completion of each layer, a roller refreshes the powder bed after the build plate moves down for the fabrication of the next layer. Powder fed AM is a process in which an energy source, often a laser beam, forms a melt pool on a substrate material and a nozzle injects powder into the melt pool to build a 3D component, Figure 1B. One of the most common powder fed processes is known as Directed Energy Deposition (DED). It is worth noting that powder fed processes have a variety of names, such as direct metal deposition (DMD) and laser engineered net shaping (LENS), as a result of marketing and patents. Without considering the differing methods of powder delivery for deposition, there are other differences between these techniques that influence the decision of whether to utilize one over the other. Table 1 details some of the important features and specifications associated with each technique.

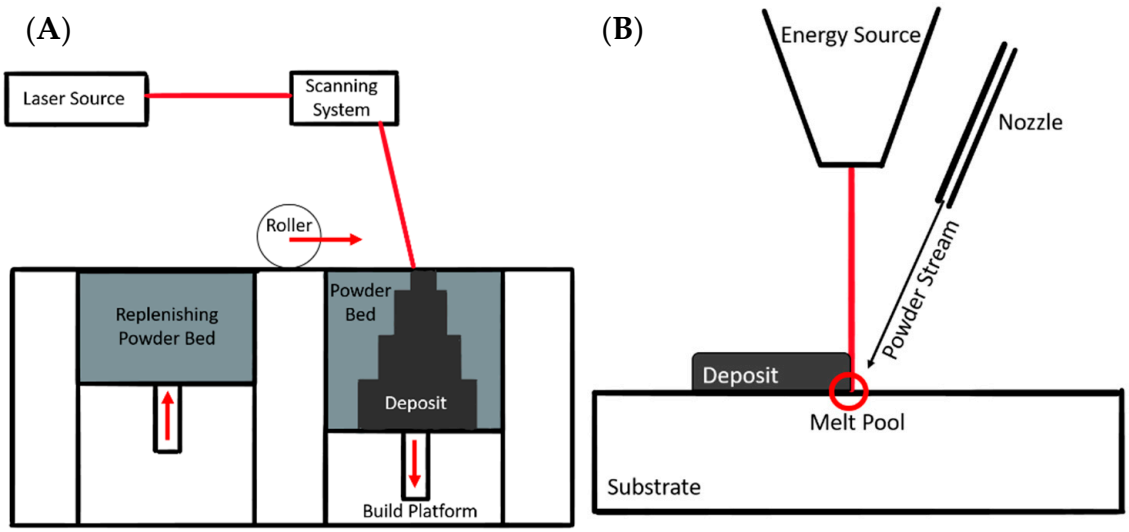

Figure 1. (**A**) Process schematic for selective laser melting (SLM), (**B**) Process schematic for directed energy deposition (DED).

Table 1. Comparison of SLM and DED processes.

Specification	Selective Laser Melting	Directed Energy Deposition
Energy Source	Laser Beam	Electron Beam, Laser Beam
Powder Size (μm) [1]	15–45 [27]	45–150 [28]
Surface Roughness	Minimal	High, often requiring post-processing
Reported Minimum Feature Size (μm) [2]	40–200 [29]	500–3000 [29]
Available Compositions	Wide range of compositions	Few compositions due to powder availability with desired characteristics
Part Repair	No, restricted to new parts	Yes, able to build upon existing structures

[1] Particle size can vary widely depending on the parameters, equipment, and particle shape. [2] Heavily dependent on the parameter, equipment, and the intended geometry. The minimum reported feature size is not absolute and just a rough idea of where the capabilities of the process lie.

1.2. Common Aluminum Alloys

Before exploring the use of nanostructures for improving the characteristics of AM aluminum, it is beneficial to discuss the characteristics of unmodified alloys to develop a baseline. This section will touch on the typical microstructures seen with AM fabricated aluminum alloys, the disastrous defects commonly seen due to the thermal cycling and rapid cooling rates of AM, and the mechanical characteristics of these alloys.

1.2.1. Microstructural Features and Defect Characterization

The typical AM microstructure is characterized as a combination of dendritic and equiaxed grains grouped together in individual melt pool regions. Not considering the effect of remelting and thermal cycling upon fabrication of the subsequent layer, the lower portion of the melt pool contains coarse grains, such as columnar and dendritic growth, while the upper portion is composed of fine grains, typically denoted as equiaxed grains. Figure 2 shows the microstructural features of a typical aluminum alloy fabricated using DED. Upon fabrication of subsequent layers, the top region of the previous melt track is remelted, often leading to the elimination of fine grains and the development of coarse grains. Examination of the overall grain growth shows preferential growth for the coarse grains in the direction of the thermal gradient. When examining the growth characteristics of a single track melt pool in DED, growth tends to occur perpendicular to the melt pool boundary [1], Figure 2D.

As mentioned above, AM processing of high-strength aluminum alloys is plagued by defects that dramatically diminish their mechanical performance. The most common defects observed are shown in Figure 3. Porosity, Figure 3A, can be the result of gases becoming trapped during processing, vaporization of low boiling elements, and gas porosity from the feedstock itself. Lack of fusion defects, Figure 3B, are formed when there is not enough energy to fully melt the powder feedstock during processing. This can be caused by using too low of power or even if the scanning speed is so high that the energy input into the powder is not sufficient to yield full melting. Solidification cracking is a major issue seen especially with aluminum alloys in the 2XXX, 5XXX, 6XXX, and 7XXX series [6–10]. These alloys are characterized as having high mechanical characteristics, but the solidification range for these alloys, especially 2XXX, 6XXX, and 7XXX, is considerably wide [8,23,30]. For AM processing, a narrow solidification is desirable, so alloys with a wide solidification range end up experiencing considerable stresses during AM processing, often resulting in detrimental cracking. It is one of the reasons that some of these conventional aluminum alloys have been considered to be unweldable in the past. The composition of the 5XXX series results in a narrower solidification range compared with the 2XXX, 6XXX, and 7XXX series alloys and exhibits a lower tendency for cracking; however, these alloys still can experience solidification cracking [6,30].

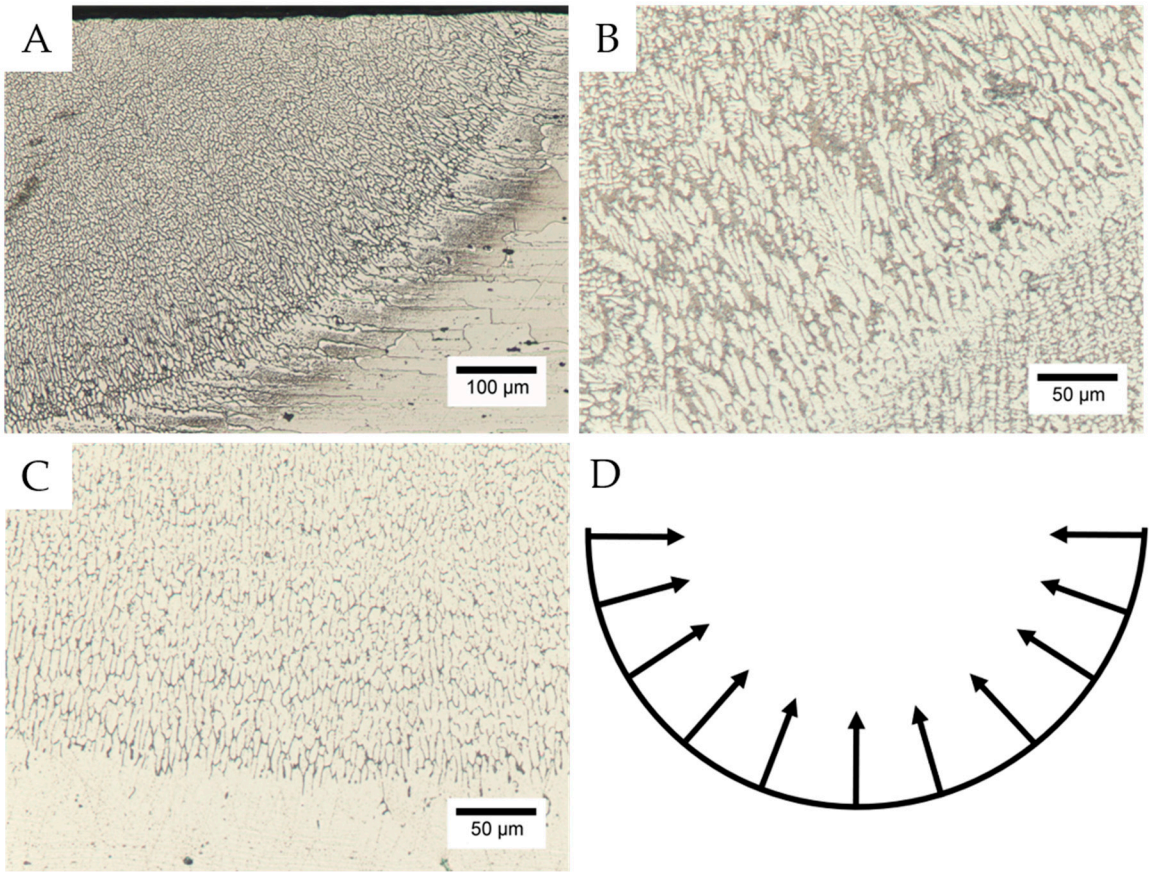

Figure 2. (**A**) Microstructural features of a melt pool of an Al 7XXX series alloy, (**B**) Dendrites at the melt pool boundary of an Al 6XXX series alloy, (**C**) Columnar growth at the melt pool boundary of an Al 6XXX series alloy, (**D**) Preferential growth diagram for a melt pool.

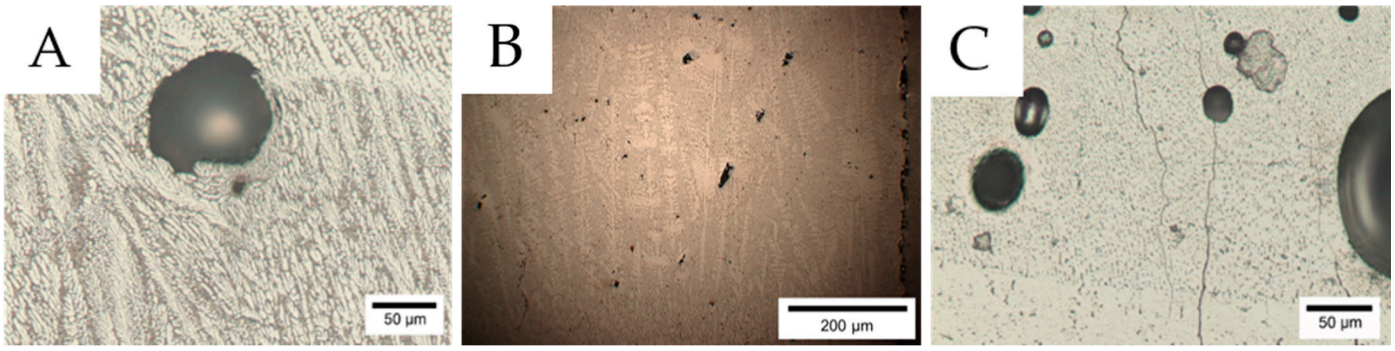

Figure 3. Defects common to AM processing. (**A**) Porosity, (**B**) Lack of fusion defects, (**C**) Solidification cracking.

Several studies have determined that high strength conventional alloys, such as 2XXX, 5XXX, 6XXX, and 7XXX series alloys, often exhibit extensive defect formation when processed through AM [6–10]. This is largely due to the fact that these alloys were not designed with AM in mind. Unlike conventional processing methods, such as casting, AM experiences rapid cooling rates and extensive thermal cycling as each layer is fabricated. As these alloys were not designed for these unique processing conditions, many of the alloy series experience detrimental stresses that eventually lead to cracking [6]. Additionally, the design process for choosing the alloying elements in conventional alloys did not consider the possibility of the processing temperatures exceeding the boiling point of some of the elements. Magnesium and zinc, two major alloying elements in aluminum alloys, have

boiling points at 1091 and 907 °C, respectively. As the processing temperatures for AM typically exceed the boiling points of magnesium and zinc, the vaporization of these elements leads to the formation of unavoidable defects [6,18–20].

In addition to the high formation of defects, aluminum alloys are plagued with issues surrounding the processing itself. Aluminum alloys exhibit high reflectivity and very low absorptivity across a wide range of laser wavelengths [21,31]. Additionally, aluminum alloys are also characterized by very high thermal conductivities, meaning that the small amount of the laser beam energy that is absorbed is quickly conducted away into the surrounding material. This is especially detrimental for DED processing which is solely dependent on the ability to form a melt pool on the substrate to enable the fabrication of a new layer. To combat this, high laser powers are often utilized, but this runs the risk of keyholing and forming additional defects, through vaporization of some of the volatile alloying elements. The processability issues are compounded by the high tendency for oxide formation associated with aluminum. Oxide films present on the powder feedstock, substrate, or the deposit can negatively impact wettability and can hinder the ability to form a stable melt pool in DED processes and remelt the previous layer in both DED and SLM [32]. Along with the complications brought on by the absorptivity and conductivity, the lightweight nature of aluminum also creates issues with powder flowability in DED and spreadability in SLM. These factors have labeled aluminum as having poor processability.

Overall, conventional aluminum alloys are plagued by processing issues and high defect formation as the alloys were not designed for the processing conditions that AM subjects them to. As this is the case, there are very few opportunities through which these issues can be addressed and resolved. Many investigators used to believe that the way to improve the process lied in the optimization of the parameters; however, the consensus is changing and the case is now being made that changing parameters alone cannot fix all of the problems [7,10,23]. As a result, the composition of aluminum alloys is being tackled on two main fronts: (1) Modification of existing alloy systems and (2) Development of new alloys.

1.2.2. Mechanical Behavior

AM fabricated aluminum alloys are typically characterized by tensile and hardness testing. The general consensus is that AM material should have properties on par or superior to their traditionally fabricated counterparts. As a result, many investigators judge the success of AM Aluminum on the ability to produce the desired mechanical characteristics. Table 2 presents a selection of mechanical properties of a range of compositions deposited using AM techniques. The majority of studies have focused on SLM as the availability of commercial equipment and powders is greater than seen for DED processes. In many cases, despite the high tendency for defect formation with conventional processes, the AM component outperforms the cast counterparts and rarely even the wrought counterparts in certain mechanical performance metrics. In addition to the conventional alloys, new alloys specially designed for AM processing are also shown. These are Scalmalloy® [33,34], an Al-Mg-Sc-Zr-based alloy, and ADDAlloy™ [35], an Al-Mg-Zr-based alloy. These alloys have shown superior properties and the capability to stand against conventional alloys known for high mechanical characteristics. It is worth noting that while Scalmalloy® shows high mechanical properties comparable to high strength aluminum alloys, such as 7075-T6, further work is required. This is largely due to the presence of scandium, a rare earth material, in the composition which has been linked to the high performance of the material [36–38]. The use of this rare earth is dependent not only on the availability, but also the cost to both the manufacturer and the end use consumer [35]. Thus, further investigation is necessary to find alternatives on par or with superior properties to this rare earth composition.

Table 2. Mechanical properties of AM fabricated aluminum alloys in the as-built condition and notable conventionally processed counterparts. YS—yield strength and UTS—tensile strength.

Material	Process	Direction	YS (MPa)	UTS (MPa)	Elongation (%)	Hardness	Source
Commercial Purity Al [1]	SLM					38 HV	[39]
	SLM	Parallel Perpendicular	90 90	110 110	30 30		[40]
Al-xCu-yMg-zMn (x = 4.24, y = 1.97, z = 0.56 wt%)	SLM		276 ± 41	402.4 ± 9.5	6 ± 1.4	111 HV	[22]
AlSi7Mg0.3 [1]	SLM		200	400	12–17		[41]
AlSi10Mg	SLM	Parallel Perpendicular		334 358	3.64 7.4	102.2 HB 103.2 HB	[42]
	SLM		196	396.5		Z: 90 HV XY: 115 HV	[43]
	DED		200 ± 10	344 ± 16	5 ± 1.0	107 ± 4 HV [2]	[44]
6061	SLM		246.7	392		Z: 67 HV XY: 84 HV	[43]
Al 7075	SLM	Parallel Perpendicular		203 ± 12 42 ± 7.5	0.50 ± 0.2 0.51 ± 0.25		[9]
Scalmalloy®	SLM	Parallel	280 ± 6.1 [2]	415 ± 14 [2]	14–17 [2]	110 ± 3 HB [3]	[33]
ScalmalloyRP0.66–4.5 [1]	SLM	Parallel 45° Perpendicular	522 507 505	536 524 529	15 14.5 13	105 HV	[34]
ADDAlloy™ (1.18 wt% Zr)	SLM	Parallel Perpendicular	221 ± 1 220 ± 3	287 ± 1 292 ± 2	25.6 ± 0.8 29.0 ± 1.6	875 MPa	[35]
ADDAlloy™ (1.57 wt% Zr)		Parallel Perpendicular	282 ± 8 290 ± 6	332 ± 2 329 ± 3	24.0 ± 1.0 25.2 ± 1.5	961 MPa	
A356—F 443.0—F 710.0—F A360—F 413.0—F 518.0—F	Sand Cast Die Cast 		82 55.16 137.9 165 144.79 193	158.6 131 220.6 317 296.48 310.3	6 8 2 4 3 5	 40 HB 60–90 HB 75 HB 80 HB 80 HB	[45]
6061—O 6061—T4 6061—T6 7075—O 7075—T6	Wrought		55 145 176 103 503	124 241 310 228 572	25–30 22–25 12–17 17 11		[46]

[1] Approximate values. [2] Values obtained over a range of scanning speeds. [3] Highest hardness value obtained over a range of scanning speeds. Scanning speed of 275 mm/s.

Mechanical testing acts on the assumption of a high-density material with minimal defects. While this might be possible using conventional alloys coupled with the conventional processing methods, the high tendency for defect formation when coupling AM and conventional alloys, discussed in Section 1.2.1, dramatically impacts the mechanical behavior. In cases in which deposition is possible with minimal defects, studies have shown that AM fabricated components often exhibited mechanical properties on par or superior to the cast counterparts. However, the benefits of AM processing methods have been proven and it now falls to addressing the compositional issues to improve the processability, microstructure, and resulting mechanical characteristics.

2. Nano Enhancement of Existing Alloys for Use with AM Processing of Aluminum Alloys

As mentioned above, aluminum alloys in the 2XXX, 5XXX, 6XXX, and 7XXX series exhibit poor processability when used with AM techniques. The 7XXX series in particular, despite being known for high mechanical properties when processed using conventional methods, experience detrimental cracks during processing that dramatically diminish their mechanical behavior. This is directly linked to the composition of the alloy coupled

with the unique processing characteristics inherent in AM. Aluminum 2XXX and 7XXX series alloys are considered to be unweldable, the 6XXX series difficult to weld, and 5XXX series weldable when using filler metals. These difficulties surrounding the weldability of conventional aluminum alloys directly compromise the processability when used with AM. These alloys are unable to withstand the rapid solidification conditions, often resulting in detrimental cracks spanning multiple layers.

In response to the poor processability issues surrounding conventional alloys, some researchers have turned to fabrication of new alloys while others have embraced modification of the existing alloys. One such modification technique that has gained considerable attention is the use of nano enhancements, such as nanoparticles [47,48], platelets [39,49], and tubes [50,51], Figures 4–6. The main theory behind the implementation of these nanostructures is the benefit of a reinforcing phase that improves processibility and results in a final component with high mechanical behavior. The processibility is improved by altering the solidification behavior, which will be discussed in the next section. Thus far, a range of nanostructure materials have been explored with multiple studies examining the use of TiB_2, TiC, and carbon nanotubes (CNT) in conjunction with conventional aluminum alloys [26,47,48,50,52–54].

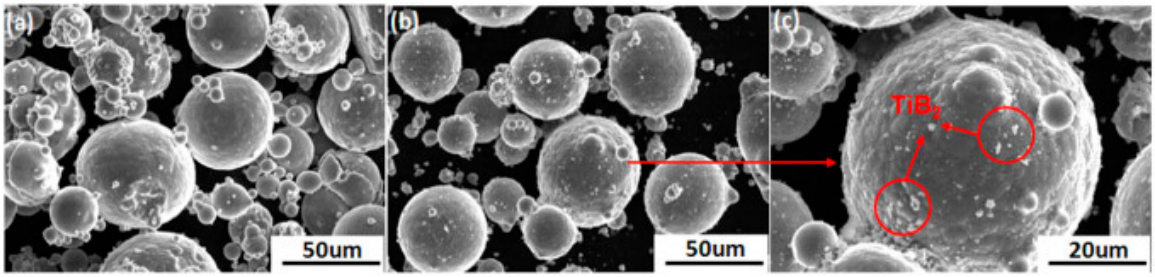

Figure 4. Powder surface morphology for unmodified and modified TiB_2/Al2024: (**a**) Unmodified, (**b**) Modified, (**c**) Modified powder showing the nanoparticles on the surface of the alloy powder. (Reprinted with permission from ref. [48]. Copyright 2019 Elsevier).

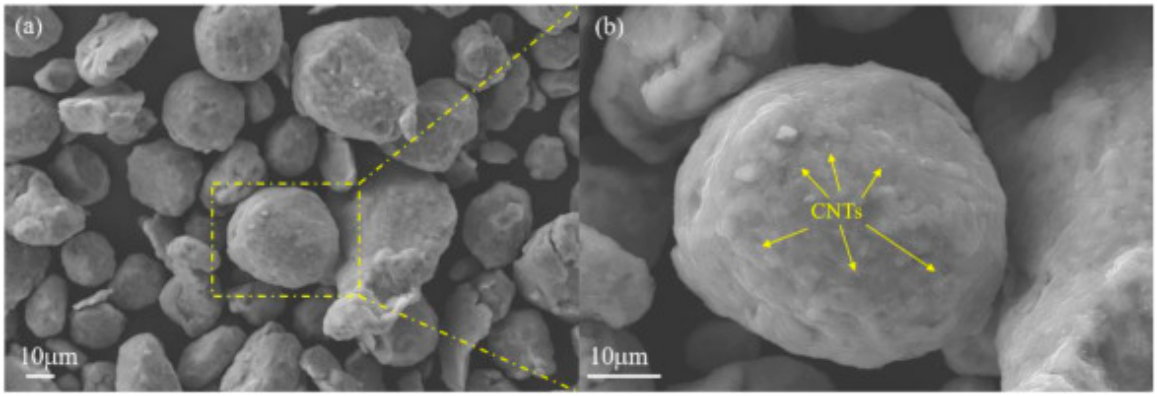

Figure 5. Powder surface morphology of an aluminum powder modified with CNTs; (**a**) Overall powder morphology, (**b**) Surface of a single particle with CNTs present on the surface. (Reprinted with permission from ref. [51]. Copyright 2020 Elsevier).

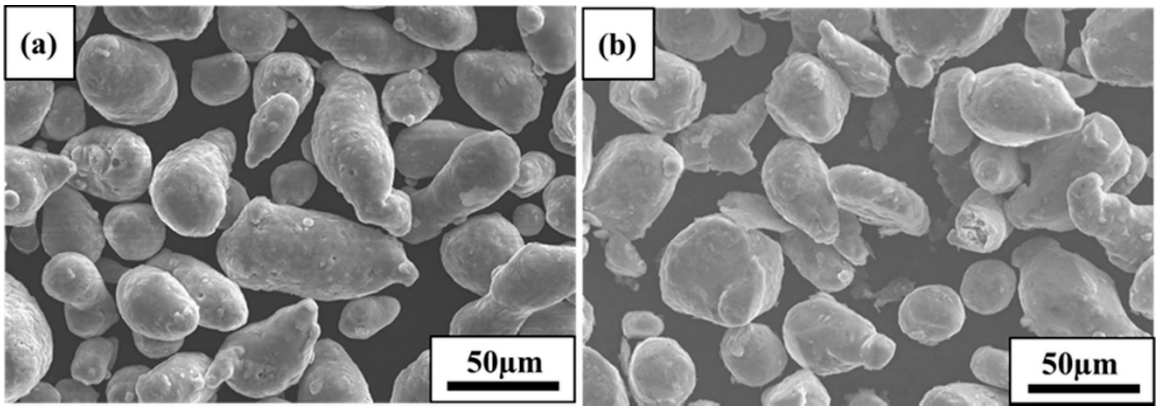

Figure 6. Aluminum powder particles, modified with graphene nanoplatelets: (**a**) Unmodified AlSi10Mg, (**b**) GNP modified AlSi10Mg. (Reprinted with permission from ref. [49]. Copyright 2020 Elsevier).

2.1. Microstructural Characteristics

Unmodified aluminum alloys that are considered to be unweldable exhibit detrimental solidification behavior when processed using AM techniques which yields final components with defects like cracks. It is worth noting that the solidification process and defect formation of AM processes are very similar to those seen with welding processes. During the solidification process, the primary equilibrium phase forms first resulting in a liquid with solute enrichment near the solidification front [8]. This creates an unstable, undercooled condition in which breakdown of the solid–liquid interface occurs, promoting cellular or dendritic growth to occur [55]. In between these grains exists the interdendritic liquid trapped between the solidified structures. These regions experience significant volumetric solidification shrinkage and thermal contraction as temperature and the amount of remaining liquid decreases [1,6,8]. The stresses that are experienced often result in solidification cracking which can propagate across many layers. In contrast, equiaxed structures are able to more easily accommodate the stresses that accompany the solidification process, preventing this cracking phenomenon that is common in dendritic and cellular structures. While equiaxed grain structures are highly desired, they are not easily obtained as the process requires a substantial amount of undercooling [55]. This is especially difficult to achieve with aluminum alloys due to the high thermal conductivities which characterize the material [55].

Nanostructures have gained traction in the AM world for their ability to alter the solidification characteristics of an alloy and enhance processability. When solidification occurs, the molten metal is only a liquid for a short period of time and as such, the possibility of interaction between the aluminum and the nanostructure reinforcing phase is minimized. The unmelted nanostructures work to inhibit grain growth and minimize the degree of undercooling needed for the formation of equiaxed grains. A lower undercooling requirement could increase the possibility of forming the desired grain structure and make the processability of unweldable or difficult to weld alloys feasible using AM processing techniques.

2.1.1. Nanoparticle Reinforcement

In processing using nanoparticle reinforcement, the nanostructures used are characterized by melting temperatures substantially higher than the melting temperature of aluminum, 660 °C. As a result, during processing, the nanoparticles do not melt and act as nucleating agents during solidification. The reinforcing particles have a similar lattice structure to aluminum and are able to reduce the barrier for heterogeneous nucleation. Wang et al. explored the use of SiC nanoparticle AlSi7Mg and at low magnification, found that both the microstructure of both unmodified and modified AlSi7Mg showed fine cellular grains, coarse cellular grains, and a transition zone [56]. However, at higher magnification,

it was found that the unmodified alloy showed fiber-like silicon while the modified alloy exhibited both silicon particles near the sub-grain boundaries and nanoparticle Al_4C_3, Figure 7 [56]. The presence of Al_4C_3 indicates that a reaction occurred between the aluminum and SiC. While the authors noted a substantial grain refinement from the addition of SiC, the texture ended up increasing by 69.60% when compared with the unmodified alloy [56].

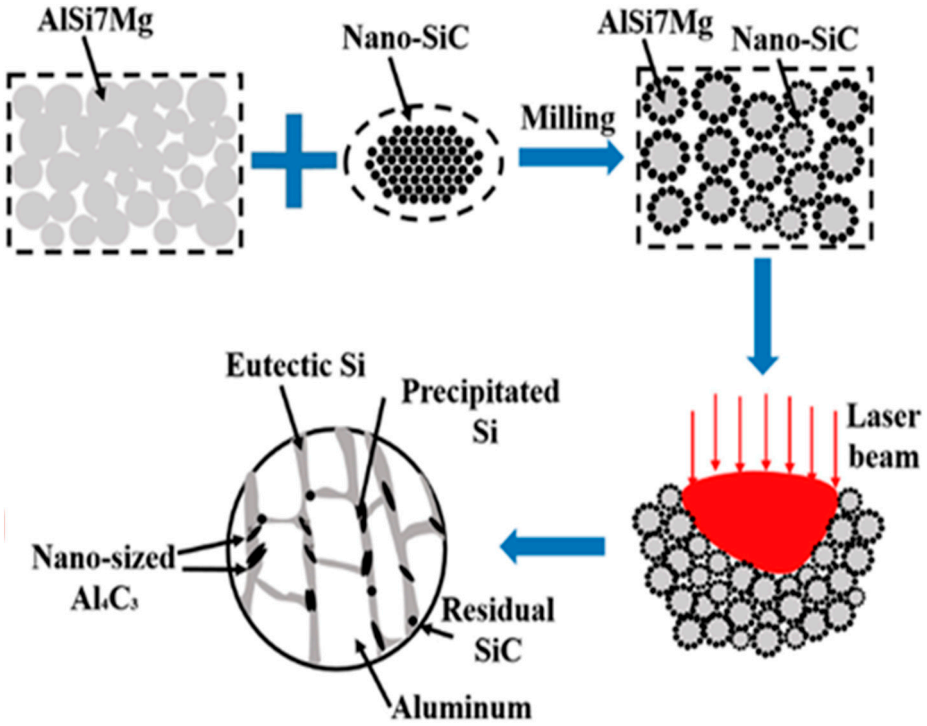

Figure 7. Reinforcement mechanisms for fabrication of aluminum alloys with nanoparticles: SiC nanoparticle reinforcement mechanism showing the eutectic silicon, nanoscale Al_4C_3, and residual SiC. (Reprinted with permission from ref. [56]. Copyright 2019 Elsevier).

Martin et al. explored the use of hydrogen stabilized zirconium nanoparticles to modify aluminum 7075 [8]. The resulting microstructure was found to be substantially different from the typical microstructure seen with unmodified 7075. The unmodified alloy exhibits large, columnar grains with extensive cracking and texture, while the addition of nanoparticle zirconium results in fine, equiaxed grains and little to no cracking [8]. The equiaxed grain structure showed minimal texture, indicating a decrease in anisotropic behavior [8]. Tan et al. used titanium nanoparticles to modify aluminum 2024 and found that the presence of the titanium lead to the formation of Al_3Ti particles during solidification, which acted as heterogeneous nucleation sites and provided grain refinement due to the small lattice mismatch between Al_3Ti and aluminum [57]. Compared to the unmodified alloy, which was characterized by large columnar grains and solidification cracks, the modified alloy showed a fine equiaxed structure with no cracking defects, Figure 8 [57].

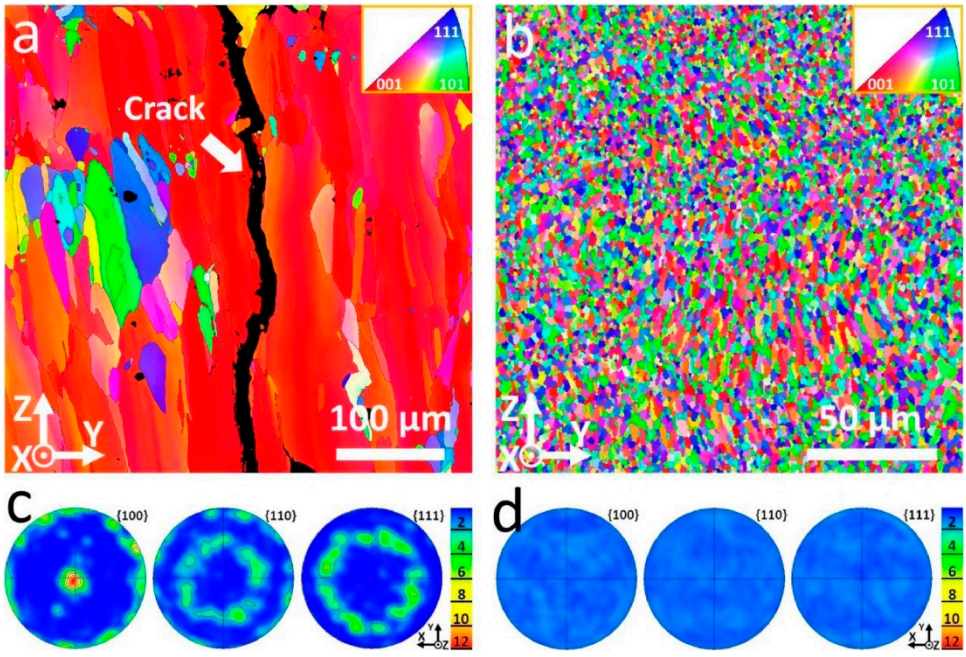

Figure 8. EBSD micrographs for modified and unmodified aluminum 2024: (**a**) Unmodified, (**b**) Modified with titanium nanoparticles. For the modified and unmodified aluminum 2024, pole figures are given in (**c**,**d**) detailing crystallographic texture in the specimens. It is clear that the unmodified specimens showed greater directionality compared to the modified alloy. (Reprinted with permission from ref. [57]. Copyright 2020 Elsevier).

Nanostructure modification of alloys for application with AM processing is a more recent avenue of investigation and as such, the microstructural response seems to be dependent on a case by case scenario and appears highly linked to the nanostructure type, nanostructure material, alloy of choice, AM processing mechanism, and the methods of production of the nanostructures. Despite this, it is worth noting the impact of the nanostructures on the microstructure that lead to the strengthening mechanisms that typically enhance the mechanical characteristics. Strengthening via nanostructure modification of an alloy can occur via four main mechanisms: grain refinement strengthening, Orowan looping, load transfer, and dislocation density strengthening due to mismatch of the coefficient of thermal expansion (CTE) [26]. It is worth noting that not all nanostructures will display these strengthening mechanisms and there is also the potential for other mechanisms depending on material factors.

Hall–Petch grain refinement is a strengthening mechanism in which strength is imparted to a material as the grain size is reduced. Nanoparticles, being effective grain refiners due to the nanoparticle acting to pin the grain boundaries coupled with the ability to act as nucleating agents and reduce the barrier for heterogeneous nucleation, promote the formation of a finer grain structure compared with unmodified alloys [58]. As a result, the Hall–Petch effect can impart strength to the final component. Orowan looping is a strengthening mechanism in which small nanosized structures obstruct dislocation motion by acting as a pinning point, forcing the dislocation to bow between two particles. From there, the bowed dislocation becomes semi-circular in shape and leaves an Orowan loop around the structure. This loop inhibits dislocation motion by increasing the difficultly of bypassing the particles. This strengthening mechanism is considered to not be applicable when considering reinforcement particles on the micron scale or larger; however, when considering the effects of nanoscale particles, Orowan strengthening tends to contribute greatly to the overall strength of the component [58]. Load transfer is a strengthening mechanism inherent to composite materials in which the bonding between the nanostructure reinforcement and the matrix alloy allows an applied load to be transferred from the matrix

to the reinforcement. This is beneficial for aluminum alloys that do not have high mechanical behavior but demonstrate good processibility with AM techniques. Thermal mismatch strengthening is a mechanism that arises during the solidification stage of processing. The CTE of the matrix and reinforcing material are often vastly different, so upon cooling, the discrepancies can result in the formation of stresses and strains in the matrix in the areas around the nanostructures [58]. Often, the stresses experienced can lead to the formation of dislocations near the nanoparticles [58].

Li et al. fabricated an AlSi10Mg composite reinforced with nano-TiB_2 particles and found that the enhancement in strength was attributed to Orowan strengthening, Hall–Petch grain refinement strengthening, and load transfer strengthening [26]. Dislocation strengthening was considered by the authors but analysis of the specimens using a transmission electron microscope determined the absence of dislocations in the regions around the nano-TiB_2 and nano-silicon particles present [26]. The authors hypothesized that the absence of dislocations was due to either the small size of the nanoparticles and their inability to create enough strain in the material or that the thermal cycling during SLM processing may have annealed out any dislocations that were present [26]. Gu et al. examined nano-TiC/AlSi10Mg components fabricated using SLM and noted that the components displayed two main strengthening mechanisms as a result of the reinforcement with nanoparticles [59]. The reinforcing phases create strengthening via grain refinement and grain boundary strengthening [59]. The grain refinement results from the presence of nanoscale reinforcing particles which inhibit the growth of the aluminum matrix grains, while the grain boundary strengthening is the result of the formation of a ring-structure from the TiC reinforcing phase [59]. The ring phase also improves the bonding between the matrix and reinforcing phase directly improving load transfer strengthening [59]. Gao et al. investigated the use of nanoparticle TiN/AlSi10Mg and noted that enhanced strength was obtained using Hall–Petch grain refinement, dislocation strengthening due to CTE mismatch, load transfer strengthening, and Orowan strengthening; the presence of TiN promoted the strengthening via Hall–Petch strengthening, dislocation strengthening, and load transfer strengthening, while the presence of silicon nanoparticles promoted Orowan strengthening [60]. TiN was not determined to be the cause of Orowan strengthening due to the low concentration of precipitates within the grains and the large spacing between TiN particles [60].

2.1.2. Carbon Nanotube and Graphene Platelet Reinforcement

The next most common reinforcement types that have been explored with AM processing of aluminum are CNTs and graphene nanoplatelets (GNPs). Both CNTs and GNPs show similar behaviors during solidification in that they both often produce Al_4C_3 phase as a side effect of the process, Figure 9. The formation of Al_4C_3 has been noted to enhance the strength of the alloy, which has gained both CNTs and GNPs considerable attention as potential reinforcement structures. During AM processing, the CNTs and graphene absorb the laser energy, first causing the structure to be destroyed and the CNTs and graphene to be partially decomposed [50]. The decomposition makes available a source of carbon, opening the potential for the formation of carbide structures, in this case Al_4C_3. Figure 8 shows the in-situ formation of Al_4C_3 from CNTs and the resulting microstructural characteristics. The use of CNTs and graphene can pose a major issue to the overall integrity of the nanostructure modified alloy as a result of the tendency for carbon to interact with the matrix material to form carbides [50]. Reports have noted that the presence of Al_4C_3 may have a negative impact on the interface characteristics of aluminum and CNTs and subsequently the strengthening behavior of the material.

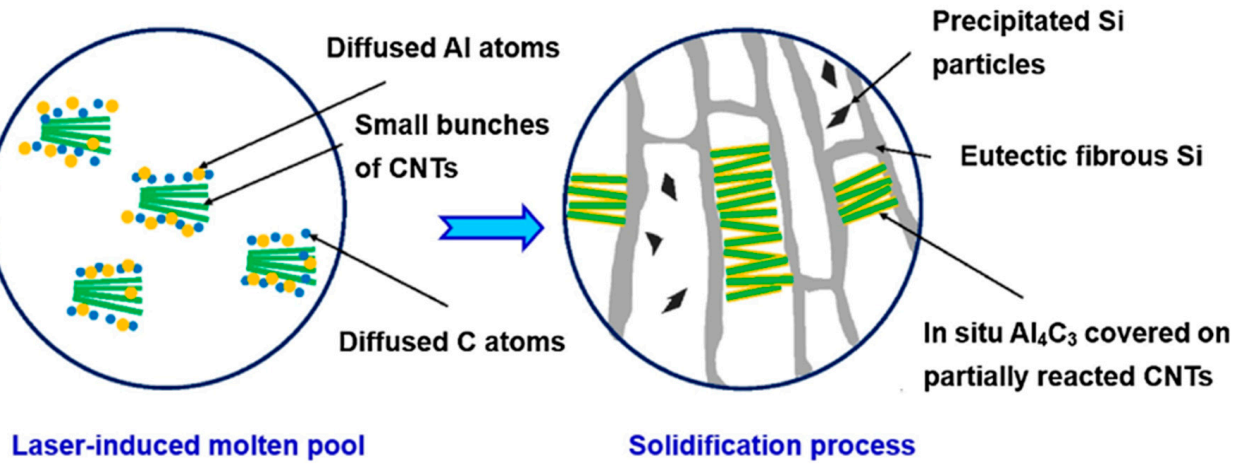

Figure 9. CNT reinforcement mechanism. (Reprinted with permission from ref. [50]. Copyright 2019 Elsevier).

In terms of the microstructure of CNT reinforcement, Gu et al. explored the use of CNTs to modify SLM fabricated AlSi10Mg and found that the microstructure was composed of 3 zones: (1) Coarse cellular, (2) Transition zone, (3) Fine cellular [50]. Of note was the features of the coarse cellular dendritic zone in which there was primary Al9Si and a fibrous web of eutectic silicon [50]. Overall, the final microstructure was similar to the typical microstructure seen with AM processing in that the cellular structures near the melt pool boundaries were coarse and grew towards the center of the track while the structure was fine near the top of the track [50]. Jiang et al. explored the fabrication of CNTs/AlSi10Mg and noted a few microstructural similarities between unmodified and modified AlSi10Mg. Both modified and unmodified alloys exhibit silicon precipitation at the cell boundaries which subsequently forms a eutectic silicon network at the boundaries; however, the modified alloy also exhibits CNTs and Al_4C_3, formed from the decomposition of CNTs when processed with the laser. CNTs and Al_4C_3 orient along the boundaries of the cells.

In terms of the microstructural behavior of the GNP reinforcing structures, Wu et al. explored the SLM fabrication of a AlSi10Mg matrix reinforced with GNP and noted the presence of a fine cellular dendritic structure in both the modified and unmodified AlSi10Mg, Figure 10a,b [49]. An enlarged image of the GNP reinforcement is visible in Figure 10c and the subsequent EDS elemental map in Figure 10d shows the successful dispersion of the reinforcing phase [49]. In addition, notable was the fact that little to no grain refinement was seen as a result of modification with GNPs [49]. Wang et al. explored the use of GNPs to reinforce SLM fabricated AlSi10Mg and found that the presence of GNPs in the composite induced extensive porosity formation [61]. The authors noted a difference in the porosities seen with unmodified and modified AlSi10Mg where the unmodified alloy shows spherical porosity and the GNP modified alloy shows irregular porosity [61]. The irregular pores are theorized to be the result of insufficient melting and a poor degree of overlap of tracks during processing [61]. However, the authors determined that more research was needed not only to understand the reasoning behind the increased porosity, but how to counteract it [61].

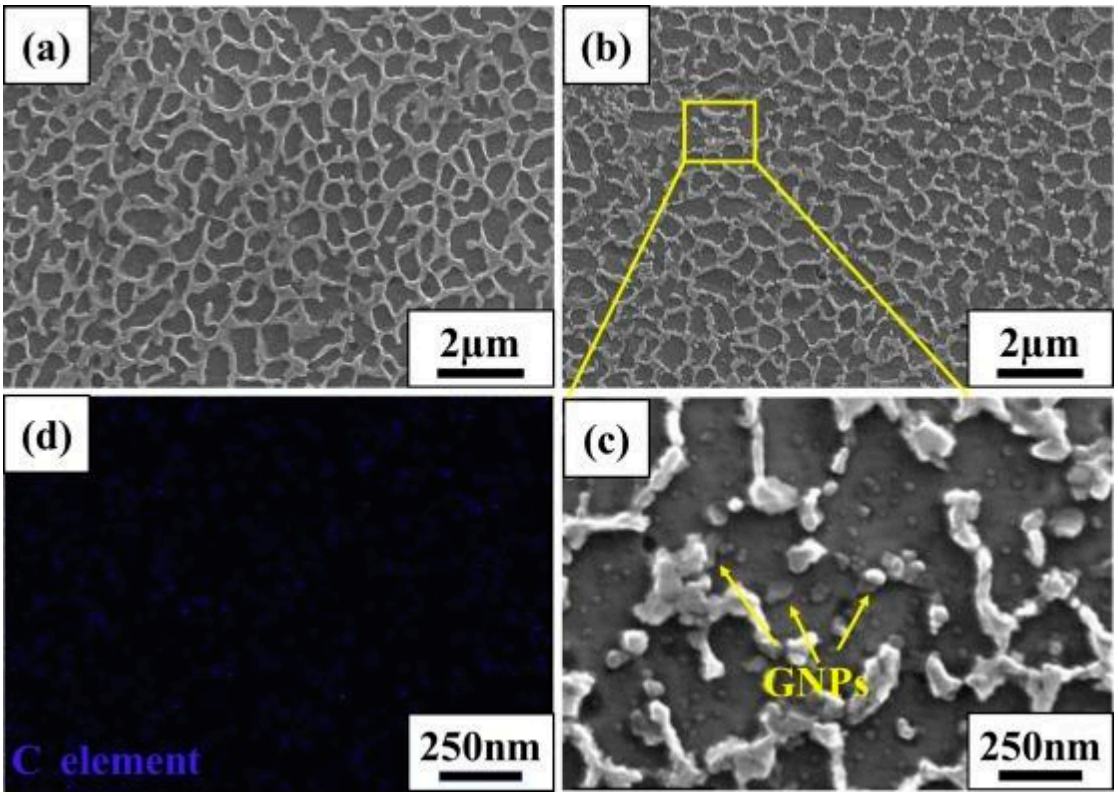

Figure 10. AlSi10Mg and GNP reinforced AlSi10Mg microstructural characteristics: (**a**) Unmodified AlSi10Mg, (**b**) GNP modified AlSi10Mg, (**c**) High magnification of GNP structures in GNP modified AlSi10Mg, (**d**) EDS elemental map of carbon. (Reprinted with permission from ref. [49]. Copyright 2020 Elsevier).

As with nanoparticles, CNTs and graphene nanoplatelets also provide potential strengthening benefits. Gu et al. noted that Orowan looping was a possible strengthening mechanism for CNT modified AlSi10Mg due to the presence of nanoscale eutectic silicon particles, precipitated silicon particles, and Al_4C_3 on partially reacted CNTs [50]. Luo et al. explored the use of CNTs to modify AlSi10Mg components fabricated by AM techniques and determined that the main strengthening mechanisms were grain refinement strengthening, secondary phase strengthening, where the structure acts as a pinning point to inhibit dislocation motion, causing the dislocations to bend between nanostructures, causing stresses that prevent any subsequent motion of dislocations, and load transfer strengthening [62]. Phase strengthening is made possible by the presence of nanoscale eutectic silicon precipitates in the aluminum and the CNTs' outer wall coated with Al_4C_3. These structures strengthen the aluminum matrix and subsequently improve overall strength. Further, the addition of CNTs to AlSi10Mg promoted the formation of Al_4C_3 on the outer surfaces of the CNTs, which improved the interface stability and worked to enhance load transfer strengthening [62]. Wang et al. explored the fabrication of CNT modified AlSi10Mg and noted enhanced strength characteristics. The authors noted that the presence of CNTs was the main contributor towards the enhancement and that the hypothesized mechanisms that acted were Hall–Petch grain refinement and dislocation pinning. Jiang et al. examined CNTs/AlSi10Mg components and noted that property enhancement was obtained through the pinning effect from CNTs and Al_4C_3 which work to enhance the silicon network and inhibit dislocation motion [54]. The authors also noted that both the uniform dispersion and good interfacial stability between the matrix and the reinforcing phase contributed to an enhancement in mechanical characteristics [54].

Wu et al. explored the use of GNP modified AlSi10Mg and noted the effects of load transfer strengthening and dislocation strengthening improved the strength and hardness relative to the unmodified alloy [49]. Wang et al. also explored GNP/AlSi10Mg and

noted the strengthening benefits of load transfer and dislocation strengthening via CTE mismatch [61]. Unlike Wu et al. [49], Wang et al. noted that Orowan strengthening played a crucial role in strengthening by hindering dislocation motion and increasing the stress needed for the dislocations to move through the component [61].

2.2. Mechanical Characterization of Nano-Enhanced Alloys

As discussed above, mechanical characterization is highly influenced by the defects present in the material. A material with many defects may yield lower mechanical properties when compared with a material with minimal defects present. As a result, it is desired to minimize the number of defects present in the final component. This section seeks to explore the notable investigations on nanostructure modified aluminum alloys.

Mechanical characterization data for nano-enhanced aluminum alloys is given in Table 3. Li et al. explored the use of TiB_2 nanoparticles for the modification of AlSi10Mg for the improvement of SLM fabricated components [26]. The authors found that the presence of the nanoparticles had a positive impact on the tensile characteristics of the material, resulting in properties higher than typically seen with SLM fabricated AlSi10Mg [26]. In addition to the enhancement of the tensile properties, the authors also found that the presence of nano-TiB_2 also had a positive impact on the laser absorptivity resulting in an increase in absorptivity of ~50% [26]. Gu et al. used nanoscale TiC to reinforce SLM fabricated AlSi10Mg and found that the tensile properties and hardness did show improvement relative to SLM AlSi10Mg not modified with nanostructures [59]. However, when the results found by Gu et al. [59] are compared with the tensile properties achieved using nano-TiB_2 found by Li et al. [26], the improvement in tensile strength from TiC was −8.3% and −29.7% for average ultimate tensile strength (UTS) and average elongation, respectively.

Table 3. Mechanical properties of nano-enhanced aluminum alloys fabricated via AM processing methods.

Material	Process	Direction	UTS (MPa)	Elongation (%)	Hardness	Source
4 vol% Al_2O_3/Aluminum	SLM		160	~5	48.5 HV	[63]
0.5 wt% Graphene nanoplatelets/Aluminum	SLM				47.1 HV	
1.0 wt% Graphene nanoplatelets/Aluminum	SLM				49.6 HV	[39]
2.5 wt% Graphene nanoplatelets/Aluminum	SLM				66.6 HV	
3 wt% TiB_2/A2024	DED [1]		284	18.7	108.5 HV	[48]
1 wt% Ti/A2024	SLM	Transverse	365 ± 15	12 ± 0.5		[57]
		Longitudinal	356 ± 6	12 ± 1.5		
2 wt% SiC/AlSi7Mg			502.94	10.64 ± 1.06		[56]
3.4 vol% TiB_2/AlSi10Mg	SLM	Parallel	529.60 ± 4.58	7.53 ± 0.15		[52]
		Perpendicular	522.91 ± 3.59	8.68 ± 0.49		
7 vol% TiB_2/AlSi10Mg			530 ± 16	15.5 ± 1.2	191 ± 4 $HV_{0.3}$	[26]
3 wt% TiC/AlSi10Mg	SLM		486	10.9	188.3 HV_{01}	[59]
2 wt% TiN/AlSi10Mg	SLM				145 $HV_{0.1}$	[64]
0.5 wt% Graphene nanoplatelet/AlSi10Mg	SLM		346	3.2		[61]
1 wt% Carbon Nanotubes/AlSi10Mg	SLM		499	7.6	143.33 HV	[54]
0.5 wt% Carbon Nanotubes/AlSi10Mg	DED		89.0 [2]		105.8 $HV_{0.1}$	[53]
1 vol% ZrH_2/A7075 (T6)	SLM		383–417	3.8–5.4		[8]

[1] Laser solid forming. [2] Represents the increase in UTS achieved from adding 0.5 wt% carbon nanotubes to AlSi10Mg relative to unmodified AlSi10Mg.

In addition to modification with nanoparticles, other structures have been investigated to enhance the characteristics of deposited AlSi10Mg. Wang et al. explored the use of graphene nanoplatelets for the reinforcement of AlSi10Mg [61]. The resulting deposits were found to have extensive amounts of porosity which significantly impacted the tensile properties and any potential benefits of adding graphene [61]. However, the authors noted that despite the reduction in strength brought on by the presence of porosity, the potential the graphene nanoplatelets pose for strengthening is great and further exploration should be done to find a way to minimize the formation of pores in the material [61]. In addition to reinforcement with platelet structures, studies have branched out to explore the use of CNTs for the enhancement of AM fabricated AlSi10Mg. Jiang et al. used 1 wt% CNTs with

SLM fabricated AlSi10Mg and found that the UTS and hardness exhibited improvement relative to unmodified AlSi10Mg, 20% and 10%, respectively [54].

While the majority of studies have been conducted using Al-Si-based 4XXX series alloys, the concept of nanostructure modification has begun to be applied to more difficult-to-process aluminum alloys and pure aluminum. Hu et al. investigated the impact of graphene nanoplatelets on pure aluminum and found that the addition of the graphene had a positive impact on the hardness [39]. In comparison with pure aluminum, 0.5 wt%, 1.0 wt%, and 2.5 wt% graphene nanoplatelets increased the hardness by 23.95, 30.53, and 75.26%, respectively [39]. The authors noted that while it seems that the addition of more nanoplatelets may further increase the hardness, this is not actually true as an agglomeration of the nanoplatelets would counteract the benefits achieved by adding more nanoplatelets and cause a reduction of hardness [39].

Wen et al. investigated modified A2024 with nanoparticle TiB_2 processed by laser solid forming, a subset of DED, and found that the resulting mechanical properties far surpassed the properties seen with conventionally processed A2024 [48]. The addition of TiB_2 nanoparticles resulted in a 44.6% and a 75% increase in average microhardness relative to the average for AM A2024 and cast A2024, respectively [48]. Additionally, the presence of TiB_2 nanoparticles also had a positive impact on the yield strength (~81% increase), tensile strength (~41% increase), and elongation (~167% increase) relative to AM fabricated A2024 [48]. This is a big step forward for AM of aluminum alloys as 2XXX series aluminum alloys are considered difficult to weld and possess a high degree of difficulty when fabricating with AM techniques. Martin et al. explored the benefit of using 1 vol% hydrogen stabilized zirconium with aluminum 7075 [8]. Aluminum 7075, being part of the 7XXX series, is characterized as unweldable and has been shown in many studies to be prone to solidification cracking when processed with AM techniques. The addition of hydrogen stabilized zirconium lead to the formation of Al_3Zr precipitates which acted as nucleating agents during the solidification process [8]. This resulted in a deposit with little to no solidification cracks contrary to what is typically seen with AM fabricated 7075 [8].

Overall, alloys modified with nanoparticles tend to exhibit the greatest enhancement in mechanical properties, yielding superior tensile strength, elongation, and hardness. Modification with CNT resulted in a moderate enhancement of tensile strength and elongation. Graphene platelets provided the least enhancement of the mechanical properties determined to be a side effect of the large amount of porosity present in the graphene modified components.

2.3. Property Performance of Nanoparticle Alloys Relative to New Alloys Designed for AM

Researchers have drawn the conclusion that processing many conventional aluminum alloys via AM methods cannot be done just by simply optimizing processing parameters [7,23]. The composition of the alloy is crucial to their behavior during processing and during mechanical testing. As a result, both researchers and industry have undertaken the task of addressing the problematic issue of alloy composition into two main avenues of investigation: (1) Fabrication of new alloys designed for AM and (2) Modification of existing conventional alloys to improve processability, minimize defect formation, and promote superior mechanical behavior. As these two main avenues both show considerable promise [8,34–36,38,47,49,50,65,66], it is beneficial to examine the microstructural and mechanical behavior of each method.

Solidification characteristics of an alloy in question are critical for AM processes as it directly impacts both the microstructural and mechanical characteristics. As with the modification of nanostructures, the new alloys being developed to work with AM processing also are closely linked with solidification behavior. Scalmalloy®, being an Al-Mg-Sc-Zr-based alloy, relies heavily on the rapid cooling rate to obtain a supersaturated solid solution. Upon post-processing of the alloy, fine Al_3Sc precipitates are formed which are highly coherent with the aluminum matrix. Additionally, Al_3Sc precipitates can act as nucleation sites for heterogeneous nucleation of aluminum grains promoting grain

refinement [32]. The resulting microstructure of a Scalmalloy® component displays a bimodal grain morphology with coarse grains, caused by the lack of Al_3Sc nucleation sites and a temperature gradient promoting the formation of columnar growth, and fine grains, that are promoted by the presence of Al_3Sc nucleants. Scalmalloy® has showed considerable promise for use with AM processing and the ability to fabricate components with high mechanical properties; however, there is a major downside to this alloy that must be addressed. Scandium is a rare earth element which, despite being able to yield precipitate structures with a high degree of coherency with aluminum, can be costly. Additionally, full-scale industrial use of Scalmalloy® is hindered by the price and the unstable nature of the scandium supply which could lead to rapid changes in cost. ADDAlloy™, being an Al-Mg-Zr-based alloy that does not contain costly scandium, first solidifies Al_3Zr precipitates, which act as a nucleating phase for the growth of FCC-aluminum grains. The use of Al_3Zr as a nucleant provides a strong grain refinement which results in a region of fine equiaxed grains. As seen with Scalmalloy®, ADDAlloy™ has also shown a bimodal grain structure. ADDAlloy™, like Scalmalloy® shows high mechanical properties, as a result of strengthening mechanisms linked to the presence of Al_3Sc [35]. However, while ADDAlloy™ shows promise as a scandium-free alternative, when directly compared with Scalmalloy®, refer to Table 2, ADDAlloy™ falls short in mechanical performance, indicating that more testing and process optimization is required [35].

In terms of microstructural features, nanostructure modified alloys do not show a definite trend of features like the bimodal grain distribution seen with both Scalmalloy® and ADDAlloy™ and is likely a result of several different factors: equipment, processing parameters, reinforcement material, reinforcement structure, matrix material, preparation/fabrication method of nanostructure modified alloy feedstock powder. However, both the nanostructure modified alloys and the newly designed alloys may utilize similar strengthening mechanisms as a result of the presence of nanoscale structures in each [33,35,36,67]. In terms of mechanical behavior, the nanostructure modified alloys typically show higher strength than ADDAlloy™; however, the modified alloys are on par with the strengths seen with Scalmalloy®, Figure 11. This is not the case with elongation in that both Scalmalloy® and ADDAlloy™ display considerably higher elongation values compared with the nanostructure modified alloys. From this, it can be concluded that in terms of strength, the use of modified alloys is promising, but this comes at the cost of the ductility of the material. If this avenue of material design is to be pursued, then it is necessary to address the poor mechanical elongation.

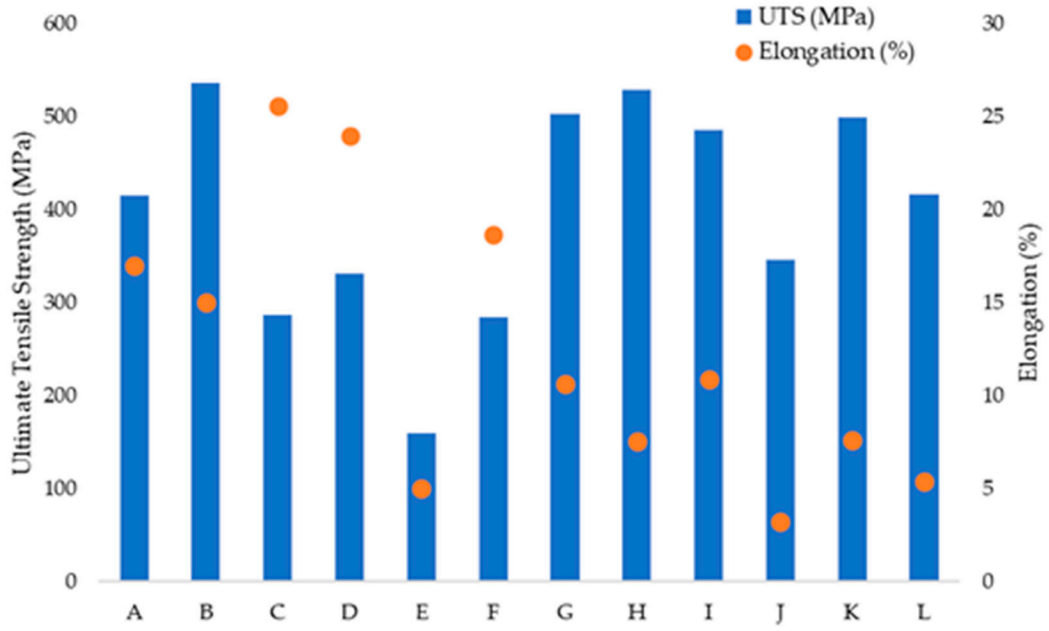

A—Scalmalloy® [33]
B—Scalmalloy®; 0° [34]
C—ADDAlloy™ (1.18% Zr); 0° [35]
D—ADDAlloy™ (1.57% Zr); 0° [35]
E—4 vol% Al_2O_3/Aluminum [63]
F—3 wt% TiB_2/A2024 [48]
G—2 wt% SiC/AlSi7Mg [56]
H—3.4 vol% TiB_2/AlSi10Mg [52]
I—3 wt% TiC/AlSi10Mg [59]
J—0.5 wt% GNPs/AlSi10Mg [61]
K—1 wt% CNT/AlSi10Mg [54]
L—1 vol% ZrH_2/A7075 [8]

Figure 11. UTS and elongation of various nanostructure modified AM fabricated aluminum alloys in comparison with Scalmalloy® and ADDAlloy™, two alloys specifically designed for use with AM processing.

3. Challenges and Future Outlook

Nanostructures show considerable promise for the advancement of AM fabricated aluminum alloys. As noted by some of the studies discussed above, the use of nanostructures has shown considerable improvements in laser absorption compared to the unmodified alloys. As laser absorption plays a crucial role in the formation of a melt pool in AM processes, the presence of nanostructures improves processibility. The presence of nanoparticle enhancements works to inhibit grain growth, promoting equiaxed grain structures; however, it is worth noting that both the reinforcement particles as well as the AM processing itself impact the actual ability to form equiaxed structures. This is specifically seen with remelting of previous layers for the fabrication of a new layer. The additional thermal cycling often negatively impacts the grain morphology and typically promotes large columnar grains. Martin et al. obtained a fine equiaxed grain structure with little to no texture despite thermal cycling through the use of aluminum 7075 modified with nanoparticle hydrogen stabilized zirconium [8]. This success shows the potential for counteracting grain growth and fabricating components with fine equiaxed structures. Nanostructures also promote strengthening mechanisms to yield high performance final components. As with any process, there are challenges that stand in the way of large-scale implementation of nanostructure-modified aluminum alloys.

3.1. Additive Manufacturing

A major issue that impacts the ability to fabricate high-performance nanostructure modified alloys is the AM process itself. Laser-based AM processes rely on the ability to melt the feedstock material to form new layers of a final component; however, the number of conventional aluminum alloys that do not have inherent and substantial processing difficulties is limited. As seen with aluminum, there are several materials that exhibit high reflectivity, such as copper, and are also coupled to high thermal conductivities, making it

difficult to form a stable melt pool. Laser-based AM processes rely on the ability to melt the feedstock material to form new layers of a final component, so issues with reflectivity and thermal conductivity will negatively impact processability.

In addition to processing difficulties, the AM process promotes unique defect formation. Alloys designed for conventional processing typically utilize lower boiling elements that are often vaporized when processed using AM techniques. The loss of these low boiling elements can lead to the formation of porosity in the components and negatively affect the mechanical behavior. Aluminum 5XXX series alloys use magnesium as the primary alloying elements. The magnesium in the 5XXX series promotes strengthening mechanisms, so a loss of this vital element can directly impact the final mechanical behavior. In some cases, the modification of the chemical composition caused by vaporization can increase the susceptibility of a material to cracking [32]. Residual stresses also play a considerable part in AM processing. The unique thermal profile resulting from thermal gradients and thermal cycling during remelting of the previous layer causes extreme stresses in the component which in some cases can result in crack formation [68]. Another major challenge that plagues AM processing is anisotropy in a single part and variation between parts. AM being a layer-by-layer process tends to promote directionality particularly along the build direction. This means that the microstructure and mechanical properties tend to show different behavior along the build direction than seen perpendicular to the build direction [68]. This creates substantial anisotropy in a single component and can limit the applications for use to ones that only require superior properties in a single direction.

3.2. Nanostructure Dispersion and the Impacts on Processing

To be an effective reinforcement, nanostructures must be well dispersed; however, it can be extremely difficult to achieve a uniform distribution of the reinforcement. Nanostructures tend to agglomerate together due to van der Waals forces between the structures that lead to inhomogeneity in the microstructure [59]. Nanocomposite materials have been fabricated using a range of conventional processes, often casting and powder metallurgy methods; however, in each method, the overall goal is to modify the matrix alloy powder with the reinforcing material in such a way that the microstructure of the final component after processing shows a dispersed nanostructure reinforcement in the matrix.

In terms of nanostructure-modified aluminum alloys, several different conventional processing methods have been employed to fabricate nanocomposites, including powder metallurgy [69,70] and stir casting [71,72]; however, dispersion remains an issue in many cases. Kuzumaki et al. explored the use of hot press and hot extrusion methods for the fabrication of CNT reinforced aluminum composites and found the mechanical properties of the reinforced materials suffered greatly and that the tensile strength was nearly identical to that of the unmodified aluminum alloy [70]. The authors determined that this was the result of poor dispersion and that in order to achieve good dispersion and subsequently enhancement relative to the unmodified alloy, a method to prevent agglomeration was required [70]. In response to the many issues with dispersion, conventional processing turned to the development of methods to disperse the nanostructures. In many cases, the dispersion method of choice is a milling process; however, this can cause damage to the matrix powder or the reinforcement phase, especially in the case of CNTs [73]. Other possible dispersion methods are proposed in conventional processing, such as ultrasonic dispersion, use of dispersants (more commonly seen with ceramic and polymer matrix composites), and liquid state mixing [73–76]. It is worth noting that there are several other methods that can be used but are not currently under AM-related research creating a vast set of possibilities to aid in dispersion.

As an alternative to traditional manufacturing techniques, AM is considered a promising option for the fabrication of nanocomposites due to the ability to fabricate components with complex geometries, limited wasted materials, and the ability to form fully functional components in a single manufacturing step compared to the multi-process steps seen with several conventional processing methods. However, like conventional processing meth-

ods, the dispersion can be particularly difficult to achieve with SLM and DED processing methods. Gu et al. explored the fabrication of nano-TiC and AlSi10Mg components and found that the nanoscale TiC reinforcing particles demonstrated a high tendency towards the formation of clusters as a result of agglomeration [47]. Hu et al. studied the interactions between graphene nanoplatelets and pure aluminum and noted the presence of agglomeration of graphene nanoplatelets when the amount of nanoplatelets exceeded 2 wt% [39]. Similar behavior has been noted with CNTs as a result of the high aspect ratio; however, researchers have shown that the use of mechanical alloying can crush the agglomerated CNTs and disperse them uniformly [50]. The use of mechanical alloying to disperse the CNTs can have a negative impact on the alloy powder and cause deformation as well as compromise the structural integrity of the CNTs if the powder overheats during milling [50].

When using AM processing for the fabrication of nanocomposites, it is worth noting that it is not just the process itself, but also the feedstock material that is important. As a result, great care is required in the preparation of the feedstock materials and consideration as to what method to fabricate the nanostructure modified feedstock powder is mandatory. Mechanical alloying via ball milling [39,77] has been adopted in many studies for the preparation of the modified powder; however, with this method, there is the potential for the matrix alloy powder to be damaged or become irregular in shape [50]. It is clear that there is a need for better methods to prepare the feedstock material that does not damage the matrix alloy particles. As discussed above, there are dispersion techniques that were developed for use with conventional processing of nanostructure modified alloys that should be investigated as potential dispersion methods for use with AM processing. Until these methods are examined, whether or not they work or are applicable, the processing of AM nanostructure modified alloys cannot truly advance as dispersion is a major barrier that faces all types of manufacturing.

3.3. Safety Considerations

Nanotechnology has captured the interest of many fields due to the ability to create novel materials and components through the use and control of small scale structures; however, while the potential benefits are vast, it is important to consider the health effects from working with nanomaterials [78]. As size decreases from the macroscale to nanoscale (10^{-9} m), the characteristics of the material itself change, often making the nanomaterial completely different from the large scale material [78]. These very properties, while highly desired, make nanomaterials hazardous to people [79]. In a study by Jiang et al., nanoscale oxides of aluminum, silicon, titanium, and zinc were compared with their larger scale counterparts to determine potential toxicity to three different bacteria [80]. The authors found that all nanomaterials, except for titanium oxide, exhibited greater toxicity than seen with the bulk materials [80]. The difference in behavior from the macro to nanoscale is influenced by both size and surface area [78,79]. The small size of the particles allows for the nanomaterial to be inhaled and travel to locations in the body that larger scale materials cannot [78,79]. The greater surface area of these materials increases the potential for interaction between the nanomaterial and biological cells and tissues, thereby increasing their reactivity [81]. The toxicity seen with nanomaterials coupled with the small size and large surface area poses a considerable health and safety risk to human beings [78,79].

In addition to being aware of the potential dangers associated with the small scale and large surface area of nanomaterials, it is also necessary to have an understanding of the potential routes of exposure and the associated hazards. The three most common sources of exposure are inhalation, ingestion, and skin exposure with inhalation posing the greatest risk of exposure [78,79,81]. Nanomaterials have the ability to reach all regions of the lungs and in many cases, the alveolar macrophages, responsible for removing particles from the respiratory system, are not able to remove the nanoscale materials from the body [81]. Exposure to inhalation risks can occur during the processing stage during the fabrication of the nanomaterial as well as during the use of the raw material by the end

user [79]. Skin exposure to nanomaterials has garnered considerable attention due to the risks of exposure associated with both manufacturing and use of the materials [78,79,81]. Overall, the literature on dermal exposure indicates that the small size increases the likelihood of penetration into the skin and that damaged skin is an avenue for exposure [82]. Ingestion of nanomaterials is rare but is possible through for exposure through hand to mouth contact [79,81,82]. The danger from nanomaterials is clear and proper methods of mitigating these risks must be followed before large scale deployment of nanomaterials in AM.

3.4. Future Outlook

Extensive studies are required to identify the optimal nanostructure and material that would best enhance the properties of the alloy. Not all nanostructure materials will work with every alloy composition. This is especially seen in cases where the alloy and the nanostructure are reactive with each other. While this is easy in concept, in actuality, extensive design, testing, and optimization is required which takes time and patience. As such, the implementation of nanostructure-modified alloys is hindered by the availability of knowledge and understanding of how various nanostructure compositions will interact with the chosen alloy system.

Currently, the majority of nanostructures that have been investigated are particle-based with CNTs following in second. While there is not only a vast number of potential reinforcement materials, there are also several different types of reinforcing structures that could be used in tandem with AM processing of aluminum-based alloys. Traditional metal matrix composites have used fibers, whiskers, and platelets in addition to particles and nanotubes. Further investigation into different types of nanostructures for reinforcement is required moving forward. As the majority of investigations focus entirely on particle reinforcement, there is clear potential for further improvements and enhancement of the microstructural and mechanical behavior.

In addition to further exploration into different compositions and structure types, it is believed that in the future, studies will focus on post-processing of nanostructure modified alloys. Post processes, such as heat treatments, hot isostatic pressing (HIP), and surface treatments, such as shot peening, have gained traction with both unmodified conventional alloys and new alloys designed for use with AM techniques [8]. Studies have shown that post-processing methods have enhanced the mechanical characteristics as compared to the as-fabricated components [34,35,83,84]. So far, the use of post-processes has been mostly restricted to alloys not modified with nanostructures; however, in cases where post-processing has been explored, it is clear that this is an avenue of work worth pursuing. As discussed above, Martin et al. modified aluminum 7075 with nanoparticle hydrogen stabilized zirconium that was then T6 heat treated and noted a massive improvement in microstructural and mechanical behavior relative to the unmodified alloy [8]. In the future, it is expected that the post-processing will be implemented with nanostructure modified alloys to try and enhance the behavior of the components.

Despite the clear challenges surrounding the use of nanostructures, the benefits still propel forward investigations into nanostructure modified alloys for use with AM processing. It is expected that in the future, nanostructure-modified aluminum alloys will become more commonly used than unmodified conventionally designed alloys and possibly even surpass the use of new alloys specially designed for AM processing.

Author Contributions: R.B. and S.P.I. wrote the manuscript. F.L. and S.P.I. edited the manuscript. F.L. oversaw the project. All authors reviewed the manuscript. All authors have read and agreed to the published version of the manuscript.

Funding: This research was funded by Navair STTR Phase II contract # N6833520C0029 (PM: Mr. Nam Phan) through Product Innovation and Engineering, LLC, and the Department of Education's GAANN program grant number: P200A180061.

Institutional Review Board Statement: Not applicable.

Informed Consent Statement: Not applicable.

Data Availability Statement: The data presented in this study are available within the article.

Acknowledgments: The authors would like to thank the support from Gamma Alloys for nanoparticle-enhanced aluminum powder, and Intelligent Systems Center (ISC), and Material Research Center (MRC) for the help in sample preparation and testing. The support from NSF equipment grant CMMI 1625736 is also appreciated.

Conflicts of Interest: The authors declare no conflict of interest.

References

1. Aboulkhair, N.T.; Simonelli, M.; Parry, L.; Ashcroft, I.; Tuck, C.; Hague, R. 3D printing of Aluminium alloys: Additive Manufacturing of Aluminium alloys using selective laser melting. *Prog. Mater. Sci.* **2019**, *106*, 100578. [CrossRef]
2. Introduction to Aluminum and Aluminum Alloys. In *Metals Handbook Desk Edition*, 2nd ed.; ASM International: Materials Park, OH, USA, 1998; pp. 417–423, ISBN 978-1-62708-199-3.
3. Properties of Wrought Aluminum Alloys. In *Metals Handbook Desk Edition*, 2nd ed.; ASM International: Materials Park, OH, USA, 1998; pp. 460–484, ISBN 978-1-62708-199-3.
4. *Alloying: Understanding the Basics*; Davis, J.R. (Ed.) ASM International: Materials Park, OH, USA, 2001; ISBN 9781615030637.
5. Isanaka, S.P.; Karnati, S.; Liou, F. Blown powder deposition of 4047 aluminum on 2024 aluminum substrates. *Manuf. Lett.* **2016**, *7*, 11–14. [CrossRef]
6. Mauduit, A. Study of the suitability of aluminum alloys for additive manufacturing by laser powder bed fusion. *UPB Sci. Bull. Ser. B Chem. Mater. Sci.* **2017**, *79*, 219–238.
7. Kaufmann, N.; Imran, M.; Wischeropp, T.; Emmelmann, C.; Siddique, S.; Walther, F. Influence of Process Parameters on the Quality of Aluminium Alloy EN AW 7075 Using Selective Laser Melting (SLM). *Phys. Procedia* **2016**, *83*, 918–926. [CrossRef]
8. Martin, J.H.; Yahata, B.D.; Hundley, J.M.; Mayer, J.A.; Schaedler, T.A.; Pollock, T.M. 3D printing of high-strength aluminium alloys. *Nature* **2017**, *549*, 365–369. [CrossRef] [PubMed]
9. Reschetnik, W.; Brüggemann, J.P.; Kullmer, G.; Richard, H.A.; Aydinöz, M.E.; Grydin, O.; Hoyer, K.-P.; Kullmer, G.; Richard, H.A.; Richard, H.A. Fatigue crack growth behavior and mechanical properties of additively processed EN AW-7075 aluminium alloy. *Procedia. Struct. Integr.* **2016**, *2*, 3040–3048. [CrossRef]
10. Qi, T.; Zhu, H.; Zhang, H.; Yin, J.; Ke, L.; Zeng, X. Selective laser melting of Al7050 powder: Melting mode transition and comparison of the characteristics between the keyhole and conduction mode. *Mater. Des.* **2017**, *135*, 257–266. [CrossRef]
11. Kempen, K.; Thijs, L.; Van Humbeeck, J.; Kruth, J.-P. Mechanical Properties of AlSi10Mg Produced by Selective Laser Melting. *Phys. Procedia* **2012**, *39*, 439–446. [CrossRef]
12. Brandl, E.; Heckenberger, U.; Holzinger, V.; Buchbinder, D. Additive manufactured AlSi10Mg samples using Selective Laser Melting (SLM): Microstructure, high cycle fatigue, and fracture behavior. *Mater. Des.* **2012**, *34*, 159–169. [CrossRef]
13. Prashanth, K.; Scudino, S.; Klauss, H.; Surreddi, K.; Löber, L.; Wang, Z.; Chaubey, A.; Kühn, U.; Eckert, J. Microstructure and mechanical properties of Al–12Si produced by selective laser melting: Effect of heat treatment. *Mater. Sci. Eng. A* **2014**, *590*, 153–160. [CrossRef]
14. Li, X.; Wang, X.; Saunders, M.; Suvorova, A.; Zhang, L.; Liu, Y.; Fang, M.; Huang, Z.; Sercombe, T. A selective laser melting and solution heat treatment refined Al–12Si alloy with a controllable ultrafine eutectic microstructure and 25% tensile ductility. *Acta Mater.* **2015**, *95*, 74–82. [CrossRef]
15. Buchbinder, D.; Schleifenbaum, H.; Heidrich, S.; Meiners, W.; Bültmann, J. High Power Selective Laser Melting (HP SLM) of Aluminum Parts. *Phys. Procedia* **2011**, *12*, 271–278. [CrossRef]
16. Singh, A. Additive Manufacturing of Al 4047 and Al 7050 Alloys Using Direct Laser Metal Deposition Process. Ph.D. Thesis, Wayne State University, Detroit, MI, USA, 2017.
17. Aluminum. In *Elements of Metallurgy and Engineering Alloys*; Campbell, F.C. (Ed.) ASM International: Materials Park, OH, USA, 2008; pp. 487–508, ISBN 978-0-87170-867-0.
18. Brice, C.; Shenoy, R.; Kral, M.; Buchannan, K. Precipitation behavior of aluminum alloy 2139 fabricated using additive manufacturing. *Mater. Sci. Eng. A* **2015**, *648*, 9–14. [CrossRef]
19. Brice, C.A.; Tayon, W.A.; Newman, J.A.; Kral, M.V.; Bishop, C.; Sokolova, A. Effect of compositional changes on microstructure in additively manufactured aluminum alloy 2139. *Mater. Charact.* **2018**, *143*, 50–58. [CrossRef]
20. Li, R.; Wang, M.; Yuan, T.; Song, B.; Chen, C.; Zhou, K.; Cao, P. Selective laser melting of a novel Sc and Zr modified Al-6.2 Mg alloy: Processing, microstructure, and properties. *Powder Technol.* **2017**, *319*, 117–128. [CrossRef]
21. Louvis, E.; Fox, P.; Sutcliffe, C.J. Selective laser melting of aluminium components. *J. Mater. Process. Technol.* **2011**, *211*, 275–284. [CrossRef]
22. Zhang, H.; Zhu, H.; Qi, T.; Hu, Z.; Zeng, X. Selective laser melting of high strength Al–Cu–Mg alloys: Processing, microstructure and mechanical properties. *Mater. Sci. Eng. A* **2016**, *656*, 47–54. [CrossRef]

23. Montero-Sistiaga, M.L.; Mertens, R.; Vrancken, B.; Wang, X.; Van Hooreweder, B.; Kruth, J.-P.; Van Humbeeck, J. Changing the alloy composition of Al7075 for better processability by selective laser melting. *J. Mater. Process. Technol.* **2016**, *238*, 437–445. [CrossRef]
24. Aversa, A.; Marchese, G.; Manfredi, D.; Lorusso, M.; Calignano, F.; Biamino, S.; Lombardi, M.; Fino, P.; Pavese, M. Laser Powder Bed Fusion of a High Strength Al-Si-Zn-Mg-Cu Alloy. *Metals* **2018**, *8*, 300. [CrossRef]
25. Zhang, H.; Zhu, H.; Nie, X.; Yin, J.; Hu, Z.; Zeng, X. Effect of Zirconium addition on crack, microstructure and mechanical behavior of selective laser melted Al-Cu-Mg alloy. *Scr. Mater.* **2017**, *134*, 6–10. [CrossRef]
26. Li, X.; Ji, G.; Chen, Z.; Addad, A.; Wu, Y.; Wang, H.; Vleugels, J.; Van Humbeeck, J.; Kruth, J. Selective laser melting of nano-TiB 2 decorated AlSi10Mg alloy with high fracture strength and ductility. *Acta Mater.* **2017**, *129*, 183–193. [CrossRef]
27. Anderson, I.E.; White, E.M.; Dehoff, R. Feedstock powder processing research needs for additive manufacturing development. *Curr. Opin. Solid State Mater. Sci.* **2018**, *22*, 8–15. [CrossRef]
28. *Standard Guide for Directed Energy Deposition of Metals*; ASTM F3187; ASTM International: West Conshohocken, PA, USA, 2016.
29. Chin, S.Y.; Dikshit, V.; Priyadarshini, B.M.; Zhang, Y. Powder-Based 3D Printing for the Fabrication of Device with Micro and Mesoscale Features. *Micromachines* **2020**, *11*, 658. [CrossRef] [PubMed]
30. Zhang, J.; Song, B.; Wei, Q.; Bourell, D.; Shi, Y. A review of selective laser melting of aluminum alloys: Processing, microstructure, property and developing trends. *J. Mater. Sci. Technol.* **2019**, *35*, 270–284. [CrossRef]
31. Dausinger, F. Laser welding of aluminum alloys: From fundamental investigation to industrial application. In Proceedings of the High-Power Lasers in Manufacturing, Osaka, Japan, 1–5 November 1999; Chen, X., Fujioka, T., Matsunawa, A., Eds.; SPIE: Bellingham, WA, USA, 2000; Volume 3888, pp. 367–379.
32. Aversa, A.; Marchese, G.; Saboori, A.; Bassini, E.; Manfredi, D.; Biamino, S.; Ugues, D.; Fino, P.; Lombardi, M. New Aluminum Alloys Specifically Designed for Laser Powder Bed Fusion: A Review. *Materials* **2019**, *12*, 1007. [CrossRef]
33. Spierings, A.; Dawson, K.; Uggowitzer, P.; Wegener, K. Influence of SLM scan-speed on microstructure, precipitation of Al3Sc particles and mechanical properties in Sc- and Zr-modified Al-Mg alloys. *Mater. Des.* **2018**, *140*, 134–143. [CrossRef]
34. Schmidtke, K.; Palm, F.; Hawkins, A.; Emmelmann, C. Process and Mechanical Properties: Applicability of a Scandium modified Al-alloy for Laser Additive Manufacturing. *Phys. Procedia* **2011**, *12*, 369–374. [CrossRef]
35. Croteau, J.R.; Griffiths, S.; Rossell, M.D.; Leinenbach, C.; Kenel, C.; Jansen, V.; Seidman, D.N.; Dunand, D.C.; Vo, N.Q. Microstructure and mechanical properties of Al-Mg-Zr alloys processed by selective laser melting. *Acta Mater.* **2018**, *153*, 35–44. [CrossRef]
36. Awd, M.; Tenkamp, J.; Hirtler, M.; Siddique, S.; Bambach, M.; Walther, F. Comparison of Microstructure and Mechanical Properties of Scalmalloy® Produced by Selective Laser Melting and Laser Metal Deposition. *Materials* **2018**, *11*, 17. [CrossRef]
37. Spierings, A.B.; Dawson, K.; Voegtlin, M.; Palm, F.; Uggowitzer, P.J. Microstructure and mechanical properties of as-processed scandium-modified aluminium using selective laser melting. *CIRP Ann.-Manuf. Technol.* **2016**, *65*, 213–216. [CrossRef]
38. Spierings, A.; Dawson, K.; Kern, K.; Palm, F.; Wegener, K. SLM-processed Sc- and Zr- modified Al-Mg alloy: Mechanical properties and microstructural effects of heat treatment. *Mater. Sci. Eng. A* **2017**, *701*, 264–273. [CrossRef]
39. Hu, Z.; Chen, F.; Xu, J.; Nian, Q.; Lin, D.; Chen, C.; Zhu, X.; Chen, Y.; Zhang, M. 3D printing graphene-aluminum nanocomposites. *J. Alloy. Compd.* **2018**, *746*, 269–276. [CrossRef]
40. Kimura, T.; Nakamoto, T. Thermal and Mechanical Properties of Commercial-Purity Aluminum Fabricated Using Selective Laser Melting. *Mater. Trans.* **2017**, *58*, 799–805. [CrossRef]
41. Kimura, T.; Nakamoto, T. Microstructures and mechanical properties of A356 (AlSi7Mg0.3) aluminum alloy fabricated by selective laser melting. *Mater. Des.* **2016**, *89*, 1294–1301. [CrossRef]
42. Wang, L.; Sun, J.; Yu, X.; Shi, Y.; Zhu, X.; Cheng, L.; Liang, H.; Yan, B.; Guo, L. Enhancement in mechanical properties of selectively laser-melted AlSi10Mg aluminum alloys by T6-like heat treatment. *Mater. Sci. Eng. A* **2018**, *734*, 299–310. [CrossRef]
43. Maamoun, A.H.; Xue, Y.F.; Elbestawi, M.A.; Veldhuis, S.C. The Effect of Selective Laser Melting Process Parameters on the Microstructure and Mechanical Properties of Al6061 and AlSi10Mg Alloys. *Materials* **2018**, *12*, 12. [CrossRef] [PubMed]
44. Kiani, P.; Dupuy, A.D.; Ma, K.; Schoenung, J.M. Directed energy deposition of AlSi10Mg: Single track nonscalability and bulk properties. *Mater. Des.* **2020**, *194*, 108847. [CrossRef]
45. Kaufman, J.G.; Rooy, E.L. *Aluminum Alloy. Castings: Properties, Processes, and Applications*; ASM International: Materials Park, OH, USA, 2004.
46. ASM Handbook Committee. Properties of Wrought Aluminum and Aluminum Alloys. In *Properties and Selection: Nonferrous Alloys and Special-Purpose Materials*; ASM International: Materials Park, OH, USA, 1990; Volume 2, pp. 62–122.
47. Gu, D.; Wang, H.; Chang, F.; Dai, D.; Yuan, P.; Hagedorn, Y.-C.; Meiners, W. Selective Laser Melting Additive Manufacturing of TiC/AlSi10Mg Bulk-form Nanocomposites with Tailored Microstructures and Properties. *Phys. Procedia* **2014**, *56*, 108–116. [CrossRef]
48. Wen, X.; Wang, Q.; Mu, Q.; Kang, N.; Sui, S.; Yang, H.; Lin, X.; Huang, W. Laser solid forming additive manufacturing TiB2 reinforced 2024Al composite: Microstructure and mechanical properties. *Mater. Sci. Eng. A* **2019**, *745*, 319–325. [CrossRef]
49. Wu, L.; Zhao, Z.; Bai, P.; Zhao, W.; Li, Y.; Liang, M.; Liao, H.; Huo, P.; Li, J. Wear resistance of graphene nano-platelets (GNPs) reinforced AlSi10Mg matrix composite prepared by SLM. *Appl. Surf. Sci.* **2020**, *503*, 4156. [CrossRef]

50. Gu, D.; Rao, X.; Dai, D.; Ma, C.; Xi, L.; Lin, K. Laser additive manufacturing of carbon nanotubes (CNTs) reinforced aluminum matrix nanocomposites: Processing optimization, microstructure evolution and mechanical properties. *Addit. Manuf.* **2019**, *29*, 100801. [CrossRef]
51. Yu, T.; Liu, J.; He, Y.; Tian, J.; Chen, M.; Wang, Y. Microstructure and wear characterization of carbon nanotubes (CNTs) reinforced aluminum matrix nanocomposites manufactured using selective laser melting. *Wear* **2020**, 3581. [CrossRef]
52. Xiao, Y.; Bian, Z.; Wu, Y.; Ji, G.; Li, Y.; Li, M.; Lian, Q.; Chen, Z.; Addad, A.; Wang, H. Effect of nano-TiB2 particles on the anisotropy in an AlSi10Mg alloy processed by selective laser melting. *J. Alloy. Compd.* **2019**, *798*, 644–655. [CrossRef]
53. Wan, L.; Shi, S.; Xia, Z.; Shi, T.; Zou, Y.; Li, K.; Chen, X. Directed energy deposition of CNTs/AlSi10Mg nanocomposites: Powder preparation, temperature field, forming, and properties. *Opt. Laser Technol.* **2021**, *139*, 106984. [CrossRef]
54. Jiang, L.; Liu, T.; Zhang, C.; Zhang, K.; Li, M.; Ma, T.; Liao, W. Preparation and mechanical properties of CNTs-AlSi10Mg composite fabricated via selective laser melting. *Mater. Sci. Eng. A* **2018**, *734*, 171–177. [CrossRef]
55. Stopyra, W.; Gruber, K.; Smolina, I.; Kurzynowski, T.; Kuźnicka, B. Laser powder bed fusion of AA7075 alloy: Influence of process parameters on porosity and hot cracking. *Addit. Manuf.* **2020**, *35*, 101270. [CrossRef]
56. Wang, M.; Song, B.; Wei, Q.; Shi, Y. Improved mechanical properties of AlSi7Mg/nano-SiCp composites fabricated by selective laser melting. *J. Alloy. Compd.* **2019**, *810*, 151926. [CrossRef]
57. Tan, Q.; Zhang, J.; Sun, Q.; Fan, Z.; Li, G.; Yin, Y.; Liu, Y.; Zhang, M.-X. Inoculation treatment of an additively manufactured 2024 aluminium alloy with titanium nanoparticles. *Acta Mater.* **2020**, *196*, 1–16. [CrossRef]
58. Wang, Y.; Shi, J.; Deng, X.; Lu, S. Contribution of different strengthening effects in particulate reinforced metal matrix nanocomposites prepared by additive manufacturing. *ASME Int. Mech. Eng. Congr. Expo. Proc.* **2016**, *2*, 7312. [CrossRef]
59. Gu, D.; Wang, H.; Dai, D.; Yuan, P.; Meiners, W.; Poprawe, R. Rapid fabrication of Al-based bulk-form nanocomposites with novel reinforcement and enhanced performance by selective laser melting. *Scr. Mater.* **2015**, *96*, 25–28. [CrossRef]
60. Gao, C.; Wu, W.; Shi, J.; Xiao, Z.; Akbarzadeh, A.H. Simultaneous enhancement of strength, ductility, and hardness of TiN/AlSi10Mg nanocomposites via selective laser melting. *Addit. Manuf.* **2020**, *34*. [CrossRef]
61. Wang, Y.; Shi, J.; Lu, S.; Xiao, W. Investigation of Porosity and Mechanical Properties of Graphene Nanoplatelets-Reinforced AlSi10 Mg by Selective Laser Melting. *J. Micro Nano-Manuf.* **2017**, *6*, 010902. [CrossRef]
62. Luo, S.; Li, R.; He, P.; Yue, H.; Gu, J. Investigation on the Microstructure and Mechanical Properties of CNTs-AlSi10Mg Composites Fabricated by Selective Laser Melting. *Materials* **2021**, *14*, 838. [CrossRef]
63. Han, Q.; Setchi, R.; Lacan, F.; Gu, D.; Evans, S.L. Selective laser melting of advanced Al-Al 2 O 3 nanocomposites: Simulation, microstructure and mechanical properties. *Mater. Sci. Eng. A* **2017**, *698*, 162–173. [CrossRef]
64. Gao, C.; Xiao, Z.; Liu, Z.; Zhu, Q.; Zhang, W. Selective laser melting of nano-TiN modified AlSi10Mg composite powder with low laser reflectivity. *Mater. Lett.* **2019**, *236*, 362–365. [CrossRef]
65. Griffiths, S.; Rossell, M.; Croteau, J.; Vo, N.; Dunand, D.; Leinenbach, C. Effect of laser rescanning on the grain microstructure of a selective laser melted Al-Mg-Zr alloy. *Mater. Charact.* **2018**, *143*, 34–42. [CrossRef]
66. Zhao, X.; Song, B.; Fan, W.; Zhang, Y.; Shi, Y. Selective laser melting of carbon/AlSi10Mg composites: Microstructure, mechanical and electronical properties. *J. Alloy. Compd.* **2016**, *665*, 271–281. [CrossRef]
67. Li, R.; Chen, H.; Zhu, H.; Wang, M.; Chen, C.; Yuan, T. Effect of aging treatment on the microstructure and mechanical properties of Al-3.02Mg-0.2Sc-0.1Zr alloy printed by selective laser melting. *Mater. Des.* **2019**, *168*, 107668. [CrossRef]
68. AbdulHameed, O.; Al-Ahmari, A.; Ameen, W.; Mian, S.H. Additive manufacturing: Challenges, trends, and applications. *Adv. Mech. Eng.* **2019**, *11*, 1–27. [CrossRef]
69. Sadeghian, Z.; Lotfi, B.; Enayati, M.H.; Beiss, P. Microstructural and mechanical evaluation of Al–TiB2 nanostructured composite fabricated by mechanical alloying. *J. Alloy. Compd.* **2011**, *509*, 7758–7763. [CrossRef]
70. Kuzumaki, T.; Miyazawa, K.; Ichinose, H.; Ito, K. Processing of Carbon Nanotube Reinforced Aluminum Composite. *J. Mater. Res.* **1998**, *13*, 2445–2449. [CrossRef]
71. Sajjadi, S.; Ezatpour, H.; Beygi, H. Microstructure and mechanical properties of Al–Al2O3 micro and nano composites fabricated by stir casting. *Mater. Sci. Eng. A* **2011**, *528*, 8765–8771. [CrossRef]
72. Mazahery, A.; Shabani, M.O. Characterization of cast A356 alloy reinforced with nano SiC composites. *Trans. Nonferrous Met. Soc. China* **2012**, *22*, 275–280. [CrossRef]
73. Simões, S.; Viana, F.; Reis, M.A.L.; Vieira, M.F. Microstructural Characterization of Aluminum-Carbon Nanotube Nanocomposites Produced Using Different Dispersion Methods. *Microsc. Microanal.* **2016**, *22*, 725–732. [CrossRef] [PubMed]
74. Rashad, M.; Pan, F.; Tang, A.; Asif, M. Effect of Graphene Nanoplatelets addition on mechanical properties of pure aluminum using a semi-powder method. *Prog. Nat. Sci. Mater. Int.* **2014**, *24*, 101–108. [CrossRef]
75. Rashad, M.; Pan, F.; Yu, Z.; Asif, M.; Lin, H.; Pan, R. Investigation on microstructural, mechanical and electrochemical properties of aluminum composites reinforced with graphene nanoplatelets. *Prog. Nat. Sci. Mater. Int.* **2015**, *25*, 460–470. [CrossRef]
76. Baig, Z.; Mamat, O.; Mustapha, M.; Sarfraz, M. Influence of surfactant type on the dispersion state and properties of graphene nanoplatelets reinforced Aluminium matrix nanocomposites. *Fullerenes, Nanotub. Carbon Nanostructures* **2017**, *4046*, 545–557. [CrossRef]
77. Gu, D.; Wang, H.; Dai, D. Laser Additive Manufacturing of Novel Aluminum Based Nanocomposite Parts: Tailored Forming of Multiple Materials. *J. Manuf. Sci. Eng.* **2016**, *138*, 376. [CrossRef]

78. Madhwani, K.P. Safe development of nanotechnology: A global challenge. *Indian J. Occup. Environ. Med.* **2013**, *17*, 87–88. [CrossRef]
79. Dhawan, A.; Shanker, R.; Das, M.; Gupta, K.C. Guidance for Safe Handling of Nanomaterials. *J. Biomed. Nanotechnol.* **2011**, *7*, 218–224. [CrossRef]
80. Jiang, W.; Mashayekhi, H.; Xing, B. Bacterial toxicity comparison between nano- and micro-scaled oxide particles. *Environ. Pollut.* **2009**, *157*, 1619–1625. [CrossRef] [PubMed]
81. Karakoti, A.S.; Hench, L.L.; Seal, S. The potential toxicity of nanomaterials—The role of surfaces. *JOM* **2006**, *58*, 77–82. [CrossRef]
82. Ellenbecker, M.J.; Tsai, C.S.-J. *Exposure Assessment and Safety Considerations for Working with Engineered Nanoparticles*; John Wiley & Sons, Ltd.: Hoboken, NJ, USA, 2015; ISBN 9781118998694.
83. Damon, J.; Dietrich, S.; Vollert, F.; Gibmeier, J.; Schulze, V. Process dependent porosity and the influence of shot peening on porosity morphology regarding selective laser melted AlSi10Mg parts. *Addit. Manuf.* **2018**, *20*, 77–89. [CrossRef]
84. Aboulkhair, N.T.; Maskery, I.; Tuck, C.; Ashcroft, I.; Everitt, N.M. Improving the fatigue behaviour of a selectively laser melted aluminium alloy: Influence of heat treatment and surface quality. *Mater. Des.* **2016**, *104*, 174–182. [CrossRef]